

Mortar methods for large deformation contact problems

Christian Hesch*¹ and P. Betsch**¹

¹ Universität Siegen, Paul-Bonatz-Str. 9-11, 57068 Siegen

© 2008 WILEY-VCH Verlag GmbH & Co. KGaA, Weinheim

1 Constrained semi-discrete elastic bodies

We focus on specific boundary conditions which restrict the motion of the semi-discrete elastic body. These restrictions can be characterized by geometric constraints acting on the boundary nodes of the discrete system at hand. In particular, we distinguish between Dirichlet-type boundary conditions and constraints due to contact. It suffices to consider the planar two-body contact problem (Fig. 1).

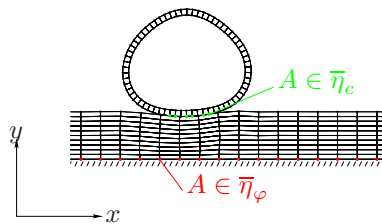


Fig. 1: The planar two-body contact problem

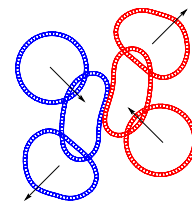


Fig. 2: Snapshots of the motion

Assume that n_{node} denotes the total number of nodes due to the space discretization of the two elastic bodies, so that $\eta = \{1, \dots, n_{node}\}$ is the set of node numbers associated with the discrete two-body system. Further let $\bar{\eta} \subset \eta$ be the set of node numbers lying on the boundaries of the two-body system. The relevant boundary conditions can be characterized by algebraic constraints of the form $\Phi(\mathbf{q}) = \mathbf{0}$. If the two bodies are in contact and provided that ‘active’ nodes $A \in \bar{\eta}_c \subset \bar{\eta} - \bar{\eta}_\varphi$ lying on the contact surface have been detected, additional constraints arise. Due to the presence of the constraints, the equations of motion can now be written in the form

$$\dot{\mathbf{q}} = \frac{\partial H}{\partial \mathbf{p}}, \quad \dot{\mathbf{p}} = -\frac{\partial H}{\partial \mathbf{q}} - D\Phi(\mathbf{q})^T \boldsymbol{\lambda}, \quad \mathbf{0} = \Phi(\mathbf{q}) \quad (1)$$

where $\Phi(\mathbf{q}) \in \mathbb{R}^m$ are the relevant constraint functions, $D\Phi(\mathbf{q})$ is the corresponding constraint Jacobian and $\boldsymbol{\lambda} \in \mathbb{R}^m$ are Lagrange multipliers which determine the size of the constraint forces in (1)₂. The set of differential-algebraic equations (DAEs) in (1) can be rewritten in compact form by introducing the augmented Hamiltonian

$$\mathcal{H}_\lambda(\mathbf{z}) = \frac{1}{2} \mathbf{p} \cdot \mathbf{M}^{-1} \mathbf{p} + \mathcal{V}_\lambda(\mathbf{q}) \quad \text{where} \quad \mathcal{V}_\lambda(\mathbf{q}) = V^{int}(\mathbf{q}) + V^{ext}(\mathbf{q}) + \boldsymbol{\lambda} \cdot \Phi(\mathbf{q}) \quad (2)$$

is an augmented potential function. Now the differential part of the DAEs can be written as $\dot{\mathbf{z}} = \mathbb{J}\nabla \mathcal{H}_\lambda(\mathbf{z})$ which, of course, has to be supplemented with the algebraic constraints (1)₃.

2 Energy-momentum scheme

We next outline the design of a time-stepping scheme which is able to reproduce for any step-size the crucial conservation properties summarized above. Concerning the time discretization of the DAEs (1), we apply the Galerkin-based approach developed by Betsch & Steinmann [1]. To this end, we consider a characteristic time-step $\Delta t = t_{n+1} - t_n$ and restrict our attention to linear approximations (the so-called mG(1) method in [1]) of the form

$$\mathbf{z}^h(\alpha) = (1 - \alpha) \mathbf{z}_n + \alpha \mathbf{z}_{n+1} \quad \text{for} \quad \alpha \in [0, 1] \quad (3)$$

In this connection all quantities at t_n , such as \mathbf{z}_n , can be regarded as being given. Note that (3) leads to a globally continuous approximation of the phase space coordinates. In contrast to that, the Lagrange multipliers are assumed to be piecewise

* e-mail: hesch@imr.mb.uni-siegen.de, Phone: +49 271 740 2101, Fax: +49 271 740 2436

** e-mail: betsch@imr.mb.uni-siegen.de, Phone: +49 271 740 2224, Fax: +49 271 740 2436

constant in each time-step, i.e. $\lambda^h = \lambda_{n+1}$. The mG(1) method yields

$$z_{n+1} - z_n = \Delta t \mathbb{J} \int_0^1 \nabla \mathcal{H}_{\lambda^h}(z^h) d\alpha \quad (4)$$

It is shown in [1] that the application of a specific quadrature formula for the evaluation of the time integral in (4) has a strong impact on the conservation properties of the resulting time-stepping scheme. In the present work we choose

$$\int_0^1 \nabla \mathcal{H}_{\lambda^h}(z^h) d\alpha \approx \bar{\nabla} \mathcal{H}_{\lambda_{n+1}}(z_n, z_{n+1}) \quad (5)$$

where $\bar{\nabla} \mathcal{H}_{\lambda}(z_n, z_{n+1})$ is a discrete gradient (or derivative) in the sense of Gonzalez [2]. It is shown in [2] that the discrete gradient can be designed such that the desired conservation properties are satisfied and specific consistency and accuracy requirements are met. To achieve this goal we aim at a reparametrization of the augmented Hamiltonian which incorporates the invariance properties in a natural way. For example, assume that the rotational invariance property holds and that the augmented Hamiltonian depends only on $\mathbb{S}(z)$, where

$$\mathbb{S}(z) = \mathbb{S}(z_1, \dots, z_N) = \{y_A \cdot y_B, 1 \leq A \leq B \leq n_{node}, y_A \in \{q_A, p_A\}\} \quad (6)$$

is the set of (quadratic) invariants of $z \in \mathbb{R}^{2n_{dof}}$. It is worth mentioning that this approach is in accordance with Cauchy's Representation Theorem (see, for example, Truesdell & Noll [5, Sect. 11.]). Accordingly, the augmented Hamiltonian can now be written in the form $\mathcal{H}_{\lambda}(z) = \tilde{\mathcal{H}}_{\lambda}(\pi(z))$. For further details on the application of this proposal to the mortar method, please refer to Hesch & Betsch [3].

3 Numerical example

The present numerical example deals with the impact of two elastic rings. Similar examples have been previously considered by Wriggers et al. [6] and Laursen & Love [4]. This example is especially well-suited to check the algorithmic conservation properties.

64 isoparametric displacement-based bi-linear finite elements have been used to discretize each initially circular ring. The material behavior of both rings is assumed to be governed by the St. Venant-Kirchhoff material model with Young's modulus $E = 100$ and Poisson's ratio $\nu = 0.1$. The mass density of both rings is $\rho_R = 0.001$. The two rings move towards each other with an initial velocity of $v_0 = 10$. In the simulations documented below a time-step of $\Delta t = 0.01$ has been used. To illustrate the simulated motion snapshots of the two rings at successive points in time are depicted in Fig. (2). After the initial free-flight phase contact takes place within the time interval of approximately [6, 16].

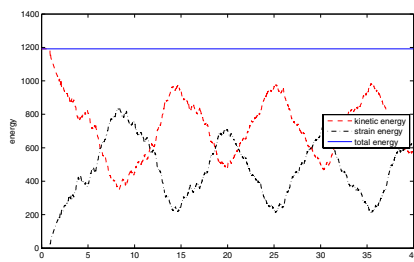


Fig. 3: Energy versus time

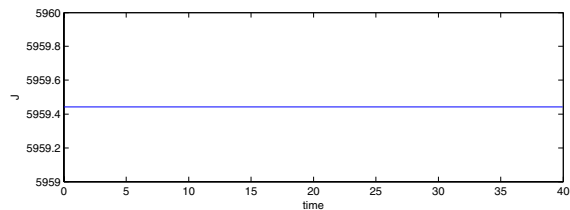


Fig. 4: Total angular momentum versus time

Since no external forces/torques act on the present two-body system the total linear momentum as well as the total angular momentum are conserved quantities. These momenta are indeed conserved by the proposed algorithm, see Fig. (4). Furthermore, algorithmic conservation of the total energy follows from Fig. (3).

References

- [1] P. Betsch and P. Steinmann. Conserving properties of a time FE method - Part II: Time-stepping schemes for non-linear elastodynamics. *Int. J. Numer. Methods Engng.*, 50:1931–1955, 2001.
- [2] O. Gonzalez. Time integration and discrete Hamiltonian systems. *J. Nonlinear Sci.*, 6:449–467, 1996.
- [3] C. Hesch and P. Betsch. Energy-Momentum Conserving Schemes for Frictionless Dynamic Contact Problems. Part II: Mortar Method. *in preparation*.
- [4] T.A. Laursen. *Computational Contact and Impact Mechanics*. Springer, 2002.
- [5] C. Truesdell and W. Noll. *The Non-Linear Field Theories of Mechanics*. Springer, 2004.
- [6] P. Wriggers, T.V. Van, and E. Stein. Finite element formulations of large deformation impact-contact problems with friction. *Computers and Structures*, 37:319–331, 1990.